

---

This is an electronic reprint of the original article.  
This reprint may differ from the original in pagination and typographic detail.

Schlee, Philipp; Tarasov, Dmitry; Rigo, Davide; Balakshin, Mikhail

**Advanced NMR Characterization of Aquasolv Omni (AqSO) Biorefinery Lignins/Lignin-Carbohydrate Complexes**

*Published in:*  
ChemSusChem

*DOI:*  
[10.1002/cssc.202300549](https://doi.org/10.1002/cssc.202300549)

Published: 22/09/2023

*Document Version*  
Publisher's PDF, also known as Version of record

*Published under the following license:*  
CC BY

*Please cite the original version:*  
Schlee, P., Tarasov, D., Rigo, D., & Balakshin, M. (2023). Advanced NMR Characterization of Aquasolv Omni (AqSO) Biorefinery Lignins/Lignin-Carbohydrate Complexes. *ChemSusChem*, 16(18), Article e202300549. <https://doi.org/10.1002/cssc.202300549>

---

This material is protected by copyright and other intellectual property rights, and duplication or sale of all or part of any of the repository collections is not permitted, except that material may be duplicated by you for your research use or educational purposes in electronic or print form. You must obtain permission for any other use. Electronic or print copies may not be offered, whether for sale or otherwise to anyone who is not an authorised user.

# Excellence in Chemistry Research

## Announcing our new flagship journal

- Gold Open Access
- Publishing charges waived
- Preprints welcome
- Edited by active scientists



## Meet the Editors of *ChemistryEurope*



**Luisa De Cola**

Università degli Studi  
di Milano Statale, Italy



**Ive Hermans**

University of  
Wisconsin-Madison, USA



**Ken Tanaka**

Tokyo Institute of  
Technology, Japan

# Advanced NMR Characterization of Aquasolv Omni (AqSO) Biorefinery Lignins/Lignin-Carbohydrate Complexes

Philipp Schlee,<sup>[a]</sup> Dmitry Tarasov,<sup>[a]</sup> Davide Rigo,<sup>\*[a]</sup> and Mikhail Balakshin<sup>[a]</sup>

*In memoriam Professor of Practice Dr. Mikhail Balakshin († 2022)*

Our recently reported AquaSolv Omni (AqSO) process shows great potential as a parameter-controlled type of biorefinery, which allows tuning of structure and properties of the products towards their optimal use in high-value applications. Herein, a comprehensive NMR (quantitative <sup>13</sup>C, <sup>31</sup>P, and 2D heteronuclear single-quantum coherence) structural characterization of AqSO lignins is reported. The effect of the process severity (P-factor) and liquid-to-solid ratio (L/S) on the structure of the extracted lignins has been investigated and discussed. Low severity (P-factor in the range 400–600) and L/S=1 led to the isolation of less degraded lignin with a higher β-O-4 content up to 34/100 Ar. Harsher processing conditions (P-factor=1000–2500)

yielded more condensed lignins with a high degree of condensation up to 66 at P-factor=2000. New types of lignin moieties, such as alkyl-aryl and alkyl-alkyl chemical bonds together with novel furan oxygenated structures have been identified and quantified for the first time. In addition, the formation of lignin carbohydrate complexes bonds has been hypothesized at low severity and L/S. Based on the obtained data we were able to formulate a possible outlook of the occurring reactions during the hydrothermal treatment. Overall, such detailed structural information bridges the gap from process engineering to sustainable product development.

## Introduction

Plant biomass is the main source of renewable chemical products and the main feedstock in biorefinery. As key products in plant biorefinery, lignin and lignin-carbohydrate hybrids are expected to play a preeminent role in various commercial applications, such as thermoplastics,<sup>[1]</sup> thermosets,<sup>[2]</sup> 3D printing,<sup>[3]</sup> carbon fibers,<sup>[4]</sup> carbon foams,<sup>[5]</sup> and carbons<sup>[6]</sup> for energy storage, among others. Considering such wide range of applications, to be technically and economically feasible, biorefineries need to consider high-value products from all biomass components, by establishing an advanced integrated biorefinery concept.<sup>[7]</sup> This new biorefinery generation shows a conceptual difference compared to the cellulose-/biofuel-/lignin first-based approaches. In this regard, our group recently published a new concept of integrated biorefinery, namely AquaSolvOmni (AqSO), where all main biomass components are treated as a source of valuable products.<sup>[8]</sup> This green, simple, and versatile approach consists in a process severity (P-factor)-driven hydrothermal treatment (HTT) of birch wood, followed by solvent (e.g., acetone) extraction of the treated solids under ambient temperature. AqSO biorefinery accounts for three major streams: hydrolysate (hemicellulose-derived products),

solvent-extracted lignin carbohydrate complexes (LCCs) and/or “pure” lignin, and cellulose-rich fibers.

Additional literature is scantily present on the isolation of lignin/LCCs through their direct alkali/solvent extraction after HTT. A pioneering work was developed by Lora and Wayman, who investigated the lignin extraction (yield up to 91.6%) with dioxane/water solutions from hydrothermally treated hardwoods ( $T=175\text{--}220\text{ }^{\circ}\text{C}$ ; liquid-to-solid ratio,  $L/S=1$ ). A mixture of dioxane/water was also used to extract lignin (26–50% yield) from steam exploded solids of aspen wood.<sup>[9]</sup> Chen and Wang produced four isolated lignin fractions from steam-exploded stalk by alkali extraction,<sup>[10]</sup> and by sequential dissolution in ethanol–water solvent.<sup>[10]</sup> Sun et al. extracted about 50% lignin from hydrothermally treated eucalyptus fiber with aqueous NaOH.<sup>[11]</sup> Our group employed aqueous acetone to extract lignins/LCCs under ambient conditions.<sup>[12]</sup> Some other works refer to the isolation of lignin/LCCs after hydrothermal treatment via hot water extraction.<sup>[7,13–20]</sup> To give some examples, a LCC-rich fraction was extracted from hot water pretreatment ( $T=130\text{--}190\text{ }^{\circ}\text{C}$ ;  $t=2\text{ h}$ ;  $L/S=10$ ) liquor of poplar wood by Feng et al.<sup>[18]</sup> Yao et al. studied the effects of process severity and pH on chemical behaviors of lignin-carbohydrate complexes extracted by hot water.<sup>[19]</sup> Giummarella and Lawoko recently developed a pressurized hydrothermal extraction ( $T=160\text{ }^{\circ}\text{C}$ ;  $t=2\text{ h}$ ) of hemicelluloses (68–75% yield) from lignocellulosic biomass (Birch and Spruce).<sup>[20]</sup>

Considering such widespread diversity of available lignins, comprehensive understanding of lignin structure is of primary importance to find the best spot for its specific applications via elucidating structure–properties–performance relationships. This would, in turn, ensure reliable product quality and predictable outcomes facilitating process upscaling. In addition, investigating the lignin structure allows to understand the

[a] Dr. P. Schlee, Dr. D. Tarasov, Dr. D. Rigo, Prof. Dr. M. Balakshin  
 Department of Bioproducts and Biosystems  
 Aalto University  
 Vuorimiehentie 1, Espoo, 02150 (Finland)  
 E-mail: davide.rigo@aalto.fi

Supporting information for this article is available on the WWW under <https://doi.org/10.1002/cssc.202300549>

© 2023 The Authors. ChemSusChem published by Wiley-VCH GmbH. This is an open access article under the terms of the Creative Commons Attribution License, which permits use, distribution and reproduction in any medium, provided the original work is properly cited.

underlying reaction mechanisms in the biorefinery processes, which is of paramount importance to unlock the full potential of complex biobased feedstocks, such as woods and grasses.<sup>[21]</sup>

The complex and irregular (amorphous) nature of lignins creates multiple issues in lignin structural analysis. To date, the combination of different nuclear magnetic resonance (NMR) spectroscopy techniques is the best method for a comprehensive elucidation of the structure of lignin. <sup>13</sup>C, 2D, and <sup>31</sup>P NMR techniques are very informative both from a qualitative and quantitative point of view. 2D NMR methods, with a focus on the heteronuclear single-quantum coherence (HSQC) technique, give good signal separation, providing reliable details on different lignin units from a semi-quantitative perspective, which in some cases showed good correlation with quantitative data.<sup>[22]</sup> It allows for the identification and quantification of very specific lignin sub-structures. However, due to very heterogeneous chemical nature of lignin (large number of moieties, each low in relative abundance), HSQC methods often report only small fractions of the lignin structure.<sup>[21]</sup> In addition, lignin moieties with quaternary carbons and specific lignin functional groups (i.e., hydroxyl groups) cannot be evaluated by the HSQC method. In contrast, <sup>13</sup>C NMR analysis can give reliable and comprehensive results on various lignin functionalities including quaternary carbon substructures, while <sup>31</sup>P NMR gives quantitative data on a few different types of OH groups in lignin.

Previous works usually focused on the NMR assignments of “traditional”, well-known lignin units, such as  $\beta$ -O-4,  $\beta$ - $\beta$ ,  $\beta$ -5, etc., and LCC linkages.<sup>[20,23–34]</sup> Despite the importance of those conventional strategies, a very comprehensive, detailed assignment and quantification of almost all lignin signals, especially in HSQC analysis is still missing. In our previous paper, we described the overall AqSO process (main streams, composition etc.) with a specific focus on the analysis of lignin carbohydrate complexes, giving little attention to other subunits/linkages and to the occurring processes/reactions during the hydrothermal treatment.<sup>[8]</sup> In addition, investigations regarding the mechanism of lignin-lignin and lignin-carbohydrates recombination and reactions are currently lacking. Hence, lignin reactions under strong acidic conditions in different reaction media have been extensively investigated<sup>[35]</sup> in contrast to the reaction of lignin and LCCs under weakly acidic and neutral conditions.

This study presents a comprehensive structural analysis of AqSO biorefinery lignins by means of different NMR techniques. The effect of process conditions, such as P-factor and liquid-to-solid ratio (L/S), on the structure of the extracted lignins was evaluated to facilitate the engineering of precursors with desirable characteristics for future applications. In addition, novel specific moieties of high importance for the lignin biorefinery, such as different type of condensed and olefinic structures, and lignin-furan-moieties have been tentatively assigned based on literature data and molecular model simulations. Such advanced structural insights enabled us to propose possible reaction mechanisms. Overall, this study may allow for an informed—rather than purely empiric—choice of process parameters for the AqSO (advanced and integrated biorefinery) process to tailor the bio-precursor properties

towards certain applications. Additionally, this comprehensive analytical approach will allow for inline product quality control by feeding artificial intelligence and machine learning driven approaches in the future.<sup>[36]</sup> These studies are currently under investigation in our group.

## Results and Discussion

The AqSO process is a versatile biorefinery concept in which the lignin structure and properties can be modified and tuned. For a detailed overview on the process itself refer to our recent paper.<sup>[8]</sup> The aim of the present work is to elucidate the structure of AqSO lignins resulting from the process and to reveal the reactions during the AqSO process by following the product formation. The advanced biorefinery concept manifested in the AqSO process requires advancement of the lignin analytics, which will be described in the following. The hydrothermal treatment (HTT) was carried out by the use of a “swing reactor”<sup>[8]</sup> and the effect of the liquid-to-solid ratio (L/S) at a fixed P-factor of 500, and of the process severity at a fixed L/S = 1 on the extracted lignin structure was investigated. Details about the products yields, their molar mass characterization, and other additional information have been reported in our recent paper.<sup>[2]</sup>

### Structure of acetone-soluble lignins (AELs)

A comprehensive NMR structural elucidation of the acetone soluble lignins (AELs) was performed by means of 2D HSQC, <sup>13</sup>C and <sup>31</sup>P analyses. The functional composition of AELs determined by quantitative <sup>31</sup>P and <sup>13</sup>C NMR can be presented in two modes: i) “as is” to understand the composition of sample in total (including carbohydrates), for correlation with properties of the samples and their performance in different applications; ii) corrected for the carbohydrate content to discuss the changes specifically in lignin and the reaction mechanism (Figures 4 and S1, Tables 3, 4, S1, and S2). For a detailed procedure on how the correction was performed refer to the experimental section.

### The effect of P-factor and L/S on key lignin units

In the course of the reaction (increasing P-factor), the syringyl-to-guaiacyl (S/G) ratio of AELs decreased from 3.6 to 2.0 (Figure 1a; Table 1, entry 1) apparently due to higher reactivity of syringyl units in lignin fragmentation in comparison to guaiacyl moieties, resulting in their predominant cleavage at the beginning of the process. Similar evidence was obtained from <sup>31</sup>P NMR data (see section 3.2.3). This phenomenon could also be attributed to higher involvement of G-units in lignin condensation and branching as compared to syringyl ones.<sup>[37]</sup> In contrast, the L/S ratio did not significantly affect the S/G ratio of AELs at a fixed P-factor of 500 (Table 2, entry 1). Noteworthy,

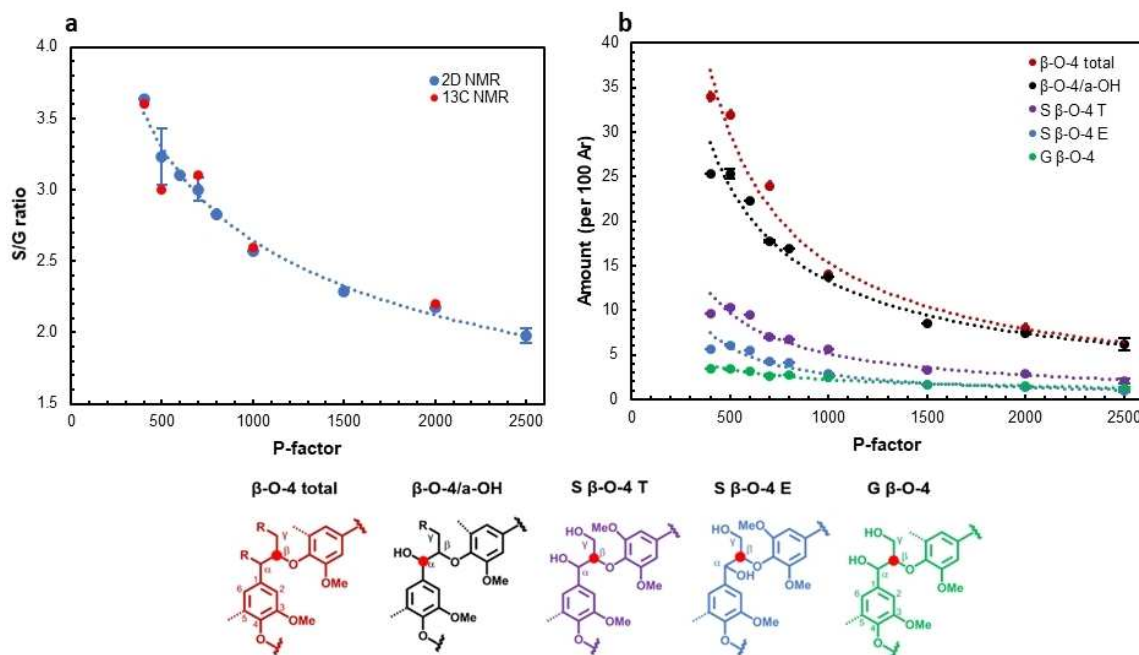


Figure 1. The effect of P-factor on the S/G ratio (a) and the amount of different  $\beta$ -O-4 moieties (b) in AELs determined by 2D HSQC NMR and  $^{13}\text{C}$  NMR.

good correlation between 2D and  $^{13}\text{C}$  NMR data for the quantification of S/G ratio was found (Figure 1a).

The quantification of  $\beta$ -O-4 linkages has been performed by both 2D HSQC and  $^{13}\text{C}$  NMR analyses. 2D HSQC allowed for the relative quantification of the total  $\beta$ -O-4/ $\alpha$ -OH amount together with the different amounts of certain isomers, like erythro/threo forms of S-type and the G-type (Figure 1b, and Table 1).<sup>[38]</sup> The total amount of  $\beta$ -O-4 bonds was evaluated by  $^{13}\text{C}$  NMR following previously reported procedures.<sup>[39]</sup> As expected, lignin degradation increased with increasing severity. This was evidenced by a significant decrease in the amounts of different  $\beta$ -O-4 moieties (Figure 1b): for instance, the total  $\beta$ -O-4 linkages decreased from 34/100 Ar to 8/100 Ar at P-factor=500 and 2000, respectively. The same trend was found for  $\beta$ -O-4/ $\alpha$ -OH linkages, showing good correlation between HSQC and  $^{13}\text{C}$  data. No effect of the L/S ratio on the  $\beta$ -O-4/ $\alpha$ -OH content (constant in the range 19–20 each 100 Ar) was detected (Table 1, entry 2), while a decrease of the total  $\beta$ -O-4 linkages from 32 to 23 each 100 Ar was observed by increasing the L/S from 1 to 2, respectively (Table 2, entry 2). This is consistent with a cleavage of  $\beta$ -O-4/ $\alpha$ -ether bonds promoted by the water in the reaction mixture. Surprisingly, little degradation of lignin occurred at L/S=1 (P-factor=500), as a high number of  $\beta$ -O-4 linkages (34/100 Ar) was still present after HTT.

The number of resinol and phenylcoumaran structures decreased during the process as well, from 7.9 and 5.1 and from 2.8 to 2 per 100 Ar at P-factor 400 and 2500, respectively (Figure 2; Table 1, entries 8–9). A neglectable effect of the L/S ratio on the variation of resinol and phenylcoumaran structures was detected (Table 2, entries 8–9).

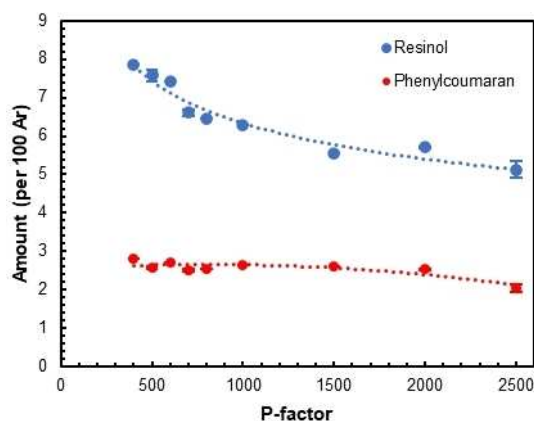


Figure 2. The effect of the P-factor on the amounts of resinol and phenylcoumaran linkages in AELs.

### New lignin moieties

The degree of lignin condensation was calculated as previously described.<sup>[31]</sup> It significantly increased with an increase in the process severity (Figure 4a and Table 3). This was obvious from the overall degree of condensation in the aromatic ring as well as from the amount of newly formed condensed moieties of alkyl-aryl (Alk-Ar) and alkyl-alkyl (Alk-Alk) types (Figure 3a, c, Figure 4a Tables 1 and 3).

In addition, AELs showed some characteristic signals in the olefinic region (Figures 3c, d, Tables 1 and 2). The exact nature of these signals is not discovered, yet. Generally, these regions were assigned as double bond with saturated aliphatic substituents (Vinyl-Alk) (in the range of ca. 125–132/5.9–

**Table 1.** The effect of P-factor at fixed liquid-to-solid ratio (L/S = 1) on the number of various moieties (per 100 Ar) in AELs by the HSQC NMR method. Only cross-peaks used for the quantification are listed. New lignin moieties have been highlighted in the table.

Entry	Moieties	Integration range ( <sup>13</sup> C/ <sup>1</sup> H)	P-factor								
			400	500	600	700	800	1000	1500	2000	2500
1	S/G ratio		3.63	3.23 ± 0.20	3.10	3.00 ± 0.08	2.83	2.57	2.29	2.18 ± 0.00	1.98 ± 0.05
2	β-O-4/α-OH	73.7–69.7/5.26–4.65	25.4	25.3 ± 0.5	22	17.8 ± 0.2	17	14	8.5	7.5 ± 0.0	6.2 ± 0.7
3	S β-O-4 T	87.7–84.8/4.04–3.85	5.7	6.1 ± 0.1	5.5	4.3 ± 0.0	4.2	2.9	1.7	1.4 ± 0.0	1.0 ± 0.2
4	S β-O-4 E	88.1–84.8/4.28–4.06	9.6	10.3 ± 0.2	9.4	7.0 ± 0.0	6.8	5.6	3.3	2.9 ± 0.0	2.0 ± 0.3
5	G β-O-4 (E + T)	84.5–82.0/4.44–4.13	3.4	3.4 ± 0.0	3.2	2.7 ± 0.0	2.7	2.4	1.7	1.5 ± 0.0	1.2 ± 0.1
6	BE total	79.0–82.0/4.5–5.1	3.8	3.5 ± 0.0	3.8	3.7 ± 0.0	3.7	3.7	3.4	3.5 ± 0.1	3.4 ± 0.0
7	α-CO/β-O-4	84.5–82.0/5.36–5.06	1.6	1.4 ± 0.0	1.5	1.4 ± 0.0	1.3	1.4	1.4	1.4 ± 0.0	1.2 ± 0.0
8	resinol	86.7–84.1/4.71–4.52	7.9	7.6 ± 0.1	7.4	6.6 ± 0.1	6.5	6.3	5.5	5.7 ± 0.0	5.1 ± 0.2
9	phenylcoumaran	89.4–85.4/5.72–5.29	2.8	2.6 ± 0.0	2.7	2.5 ± 0.0	2.5	2.6	2.6	2.5 ± 0.0	2.0 ± 0.1
10	Ar-CH=CH-CH <sub>2</sub> OH	62.6–60.5/4.17–4.06	1.4	1.0 ± 0.1	0.8	0.6 ± 0.2	0.6	0.4	0.4	0.4 ± 0.0	0.3 ± 0.0
11	Ar-CH=CH-CHO	155.5–151.8/7.75–7.46	2.7	2.1 ± 0.1	2.2	1.9 ± 0.1	1.9	1.7	1.5	1.4 ± 0.0	1.0 ± 0.1
12	Ar-CHO	192.5–189.2/10.06–9.55	4.2	3.1 ± 0.1	3.7	3.1 ± 0.3	2.9	3.2	3.1	2.8 ± 0.0	2.4 ± 0.0
13	conjugated S	109.0–103.1/7.60–6.94	11	9 ± 0.8	8.6	8.3 ± 0.4	8.2	8.3	8.5	8.4 ± 0.0	8.1 ± 0.1
14	conjugated G	126.6–121.4/7.70–7.08	6.1	6.0 ± 2.1	7.8	4.3 ± 0.0	4.5	7.6	9.8	6.5 ± 0.1	9.2 ± 0.6
15	Alk-CH <sub>2</sub> -Alk	30.0–26.9/1.37–0.69	18.0	17.3 ± 2.1	13	12 ± 1.9	12	13	13	14 ± 0.0	18 ± 0.5
16	Acetyl/3	22.2–18.9/2.15–1.68	10.1	7.0 ± 0.5	7.9	5.0 ± 0.5	4.9	4.0	2.4	2.4 ± 0.0	2.5 ± 0.3
17 <sup>[a]</sup>	γ-esters	64.6–61.0/4.43–4.21	0.7	0.4 ± 0.0	0.3	0.6 ± 0.0	0.6	0.5	0.5	0.6 ± 0.0	0.4 ± 0.0
18 <sup>[a]</sup>	GlcU Acid	98.1–96.2/5.34–5.04	1.2	0.8 ± 0.2	0.9	0.6 ± 0.0	0.5	0.3	0.1	0.1 ± 0.0	0.0 ± 0.0
19 <sup>[a]</sup>	GlcU Esters	101.5–100.0/4.72–4.59	1.2	0.8 ± 0.1	0.9	0.6 ± 0.1	0.5	0.4	0.1	0.1 ± 0.0	0.0 ± 0.0
20 <sup>[a]</sup>	PhGly	104.7–99.5/5.23–4.80	0.8	0.6 ± 0.0	0.7	0.8 ± 0.1	0.9	0.7	0.4	0.3 ± 0.0	0.2 ± 0.0
21 <sup>[a]</sup>	Term carb.		7.2	3.3 ± 0.0	7.4	5.3 ± 0.9	6.9	3.8	1.8	1.0 ± 0.0	0.5 ± 0.0
22 <sup>[a]</sup>	Internal carb.		20.4	13.9 ± 1.3	17	9.7 ± 1.1	9.3	6.6	2.4	1.7 ± 0.0	0.9 ± 0.1
23 <sup>[a]</sup>	Total carb.		27.6	17.3 ± 1.3	24	15 ± 2.9	16	11	4.2	2.7 ± 0.0	1.4 ± 0.0
24 <sup>[a]</sup>	carb. DP		3.8	5.2 ± 0.4	3.3	2.8 ± 0.1	2.4	2.7	2.3	2.7 ± 0.0	2.9 ± 0.2
25	Ar-CH <sub>2</sub> -Ar	27.8–25.2/4.06–3.93	0.0	0.1 ± 0.1	0.0	0.1 ± 0.0	0.0	0.0	0.1	0.1 ± 0.0	0.3 ± 0.1
26	Alk-Alk1	45.8–42.5/3.09–2.88	1.1	1.2 ± 0.1	1.2	1.6 ± 0.1	1.7	1.9	2.2	2.2 ± 0.0	5.2 ± 2.6
27	Alk-Alk2	51.1–46.5/2.83–2.50	0.7	1.0 ± 0.1	0.8	1.1 ± 0.0	1.2	1.4	1.9	1.7 ± 0.1	2.4 ± 0.0
28	Alk-Ar	52.5–50.3/3.72–3.53	0.6	1.6 ± 0.2	1.1	1.0 ± 0.1	1.2	0.9	0.9	1.0 ± 0.0	1.0 ± 0.3
29	Alk-Ar	50.7–46.7/3.25–3.05	0.6	0.9 ± 0.1	0.9	1.1 ± 0.1	1.2	1.3	1.7	1.7 ± 0.0	2.0 ± 0.0
30	Alk-Ar	50.0–48.1/3.45–3.27	1.1	1.3 ± 0.0	1.5	1.5 ± 0.0	1.6	1.7	1.8	1.8 ± 0.0	1.8 ± 0.1
31	Alk-Ar	49.9–43.0/3.89–3.49	0.8	1.4 ± 1.2	1.5	2.6 ± 0.5	3.3	3.0	3.8	5.1 ± 0.0	5.1 ± 1.0
32	Vinyl-Al1	127.1–123.5/6.47–5.80	4.5	4.8 ± 0.1	4.8	5.9 ± 0.2	6.0	5.4	5.1	5.9 ± 0.0	4.1 ± 0.1
33	Vinyl-Al2	133.0–127.3/6.52–5.82	8.1	8.4 ± 0.0	9.2	10.2 ± 0.4	10.6	9.4	8.6	8.2 ± 0.1	7.1 ± 0.6
34	Vinyl-Ar1	130.9–127.3/7.05–6.75	2.2	2.1 ± 0.2	1.9	1.8 ± 0.0	2.0	2.4	2.3	2.0 ± 0.0	1.7 ± 0.1
35	Vinyl-Ar2	137.2–132.4/6.75–6.54	0.4	0.6 ± 0.1	0.7	0.5 ± 0.0	0.7	0.5	0.4	0.4 ± 0.0	0.3 ± 0.0
36	Vinyl Ox	149.5–137.2/8.25–7.20	0.9	1.1 ± 0.2	0.9	1.6 ± 0.1	1.7	2.7	5.2	5.6 ± 0.0	8.3 ± 0.4
37	Fur-CHO	179.6–176.1/9.68–9.40	0.2	0.1 ± 0.0	0.2	0.2 ± 0.0	0.2	0.4	0.7	0.7 ± 0.0	1.0 ± 0.1

[a] Data taken from Ref. [8]. New lignin moieties: ■ Alkyl-alkyl. ■ Alkyl-aryl. ■ Vinyl-alkyl. ■ Vinyl-aryls. ■ Vinyl oxidized (structure F in Figure 3).

6.4 ppm)<sup>[40]</sup> and with oxygenated ones (Vinyl-Ox) (140–150/7.3–8.2 ppm). More specifically, Vinyl-Ox likely belongs to different furan moieties attached to lignin via reactions of the furan carbonyl group (see structure F, Figure 3). In addition, a characteristic signal at approx. 177.5/9.54 ppm observed in AELs was assigned to the aldehyde group in furan (furfural origin) moieties, attached to lignin via reactions in the double bonds (Fur-CHO; Figure S4). Their quantities clearly showed that the furan incorporation via carbonyl group was much more common than that via double bonds. Interestingly, the process severity did not have a significant effect on the amounts of Vinyl-Alk moieties, which were found in high amount even at the initial stage of the process (Figure 4b, Table 1). Conversely, Vinyl-Ox and Fur-CHO moieties linearly increased during the process. Surprisingly, no significant increase was observed in the amounts of carbonyl groups and saturated aliphatic moieties, which are typical products of lignin degradation.<sup>[41]</sup> Higher total degree of condensation and higher amounts of new Alk-Ar condensed moieties correlated with higher molecular mass (see molecular mass distribution in our previous paper).<sup>[8]</sup>

### <sup>31</sup>P NMR

The effect of L/S ratio on the amount of -OH and -COOH groups was very subtle (Figures 5a, c, S1, and Tables S2, S3), especially after the correction for carbohydrates. The main difference was in the extracted lignins obtained at L/S = 1; despite the highest acidity of the solution due to the lowest L/S ratio, it was less degraded as compared to AELs produced at the L/S ratios of 2–8 as indicated by higher contents of aliphatic OH and oxygenated aliphatic moieties (i.e. β-O-4 bonds, see section 3.2.1), as well as a lower amount of phenolic OH. As previously discussed, lignin degradation increased with increasing severity. It was evidenced by a significant decrease in the number of aliphatic OH (from ca. 70 to 25/100Ar at P-factors 500 and 2500, respectively) and total OH groups (from 116 to 92/100Ar at P-factors 500 and 2500, respectively) (Figure 5b and Table S3). An increase in phenolic OH (from 48 to ca. 70/100 Ar) was observed in the range of P-factor = 400–1000. However, it leveled off in the range of P-factor = 1000–2500 (Figure 5b), despite a continuous decrease in the β-O-4 moieties content (Figure 1b and Figure 1b). This may be caused by the contribution of pseudo-

**Table 2.** Effect of liquid-to-solid ratio (L/S) at fixed P-factor (500) on the number of various moieties (per 100 Ar) in AELs by the HSQC NMR method. Integration ranges are reported in Table 1.

Entry	Moieties	Liquid-to-solid ratio (L/S)			
		1 <sup>[a]</sup>	2	3	8
1	S/G ratio	3.23 ± 0.20	3.07 ± 0.05	3.07	3.01 ± 0.12
2	β-O-4/α-OH	25.3 ± 0.5	19 ± 0.1	19.1	20 ± 1.4
3	S β-O-4 T	6.1 ± 0.1	4.7 ± 0.1	4.9	5.0 ± 0.9
4	S β-O-4 E	10.3 ± 0.2	8.9 ± 0.2	8.7	9.9 ± 0.9
5	G β-O-4 (E + T)	3.4 ± 0.0	2.8 ± 0.1	2.6	2.7 ± 0.1
6	BE total	3.5 ± 0.0	3.7 ± 0.2	3.4	3.4 ± 0.2
7	α-CO/β-O-4	1.4 ± 0.0	1.4 ± 0.0	1.4	1.4 ± 0.0
8	resinol	7.6 ± 0.1	6.7 ± 0.0	6.5	6.8 ± 0.2
9	phenylcoumaran	2.6 ± 0.0	2.6 ± 0.1	2.4	2.9 ± 0.1
10	Ar-CH=CH-CH <sub>2</sub> OH	1.0 ± 0.1	0.6 ± 0.0	0.6	0.7 ± 0.1
11	Ar-CH=CH-CHO	2.1 ± 0.1	1.6 ± 0.0	1.5	1.5 ± 0.1
12	Ar-CHO	3.1 ± 0.1	2.6 ± 0.0	2.1	1.9 ± 0.4
13	conjugated S	9 ± 0.8	8.0 ± 0.0	7.4	7.9 ± 1.1
14	conjugated G	6.0 ± 2.1	4.2 ± 0.2	3.9	3.9 ± 0.2
15	Alk-CH <sub>2</sub> -Alk	17.3 ± 2.1	13 ± 0.4	12.1	11 ± 0.4
16	Acetyl/3	7.0 ± 0.5	2.9 ± 0.7	2.4	1.4 ± 0.0
17 <sup>[b]</sup>	γ-esters	0.4 ± 0.0	0.4 ± 0.0	0.4	0.3 ± 0.1
18 <sup>[b]</sup>	GlcU Acid	0.8 ± 0.2	0.4 ± 0.1	0.3	0.3 ± 0.0
19 <sup>[b]</sup>	GlcU Esters	0.8 ± 0.1	0.3 ± 0.1	0.3	0.2 ± 0.0
20 <sup>[b]</sup>	PhGly	0.6 ± 0.0	0.5 ± 0.1	0.3	0.2 ± 0.0
21 <sup>[b]</sup>	Term carb.	3.3 ± 0.0	2.6 ± 1.1	1.4	0.9 ± 0.0
22 <sup>[b]</sup>	Internal carb.	13.9 ± 1.3	6.3 ± 1.0	5.6	4.0 ± 0.1
23 <sup>[b]</sup>	Total carb.	17.3 ± 1.3	8.9 ± 2.2	7.0	4.9 ± 0.0
24 <sup>[b]</sup>	carb. DP	5.2 ± 0.4	3.8 ± 0.8	4.9	5.5 ± 0.2
25	Ar-CH <sub>2</sub> -Ar	0.1 ± 0.1	0.0 ± 0.0	0.0	0.0 ± 0.0
26	Alk-Alk1	1.2 ± 0.1	1.5 ± 0.1	1.4	1.3 ± 0.0
27	Alk-Alk2	1.0 ± 0.1	1.2 ± 0.2	1.0	1.2 ± 0.2
28	Alk-Ar	1.6 ± 0.2	1.2 ± 0.1	1.1	0.9 ± 0.1
29	Alk-Ar	0.9 ± 0.1	1.1 ± 0.1	1.0	1.0 ± 0.0
30	Alk-Ar	1.3 ± 0.0	1.6 ± 0.1	1.4	1.5 ± 0.1
31	Alk-Ar	1.4 ± 1.2	2.1 ± 0.3		1.5 ± 0.3
32	Vinyl-Al1	4.8 ± 0.1	5.7 ± 0.1	6.2	5.4 ± 0.3
33	Vinyl-Al2	8.4 ± 0.0	9.3 ± 0.3	10.8	9.6 ± 0.5
34	Vinyl-Ar1	2.1 ± 0.2	1.9 ± 0.1	2.2	1.7 ± 0.1
35	Vinyl-Ar2	0.6 ± 0.1	0.6 ± 0.0	0.8	0.7 ± 0.1
36	Vinyl Ox	1.1 ± 0.2	1.0 ± 0.1	1.1	0.8 ± 0.1
37	Fur-CHO	0.1 ± 0.0	0.2 ± 0.0	0.1	0.1 ± 0.0

[a] Data are present also in Table 1 (P-factor = 500). New lignin moieties:     Alkyl-alkyl.     Alkyl-aryl.     Vinyl-alkyl.     Vinyl-aryls.     Vinyl oxidized (structure F in Figure 3). [b] Data taken from Ref. [8].

**Table 3.** Quantitative <sup>13</sup>C analysis (per 100 Ar) of non-acetylated AELs.

P-factor	400	500	700	1000	2000	500
L/S	1	1	1	1	1	2
CO non-conjugated	8	7	11	9	17	6
CO conjugated	16	10	16	15	14	14
Total CO	24	17	27	24	31	20
COOR non-conjugated	33	18	17	12	11	12
COOR conjugated	2	2	2	2	2	2
Total COOR	35	20	19	14	13	14
OMe	162	154	146	127	116	142
S/G ratio	3.14	2.91	2.75	2.04	1.64	2.77
ArH	193	191	186	178	171	186
DC. %	31	34	40	54	66	40
β-O-4	34	32	24	14	8	23
Oxygenated Aliphatic corrected for carb.	339	258	200	134	105	176
Saturated Aliphatic	209	191	133	94	92	145
Acetyl	116	108	105	96	100	107
Carbohydrates total	22	16	8	5	5	5
internal	29	15	15	9	3	7
terminal	20	11	9	7	2	4
	9	4	6	2	1	3

lignin in the AEL mass. A similar trend was observed for S-type phenolic OH, as their number increased until P-factor = 1000, levelling off at higher severity (Figure 5d). In contrast, G- and H-type phenolics appeared to be less influenced by P-factor, suggesting that the cleavage of β-O-4 moieties might preferably occur on S-type structures, as stated above. The proportion of 5-substituted and 5-free PhOH was about the same, ca. 4:1, under all process conditions (Tables S2, S3). A two-fold increase in the number of COOH groups was observed; however, these moieties were rather minor (3.5–7/100 Ar) (Figure 5b).

### General reaction mechanisms of lignin and LCC transformation in AqSO process

Our results showed that the HTT reaction mechanisms are extremely complex. As the mechanisms of specific individual reactions cannot be addressed in detail due to the very high complexity of the whole biomass transformation, in contrast to model compounds experiments, the discussion is limited to

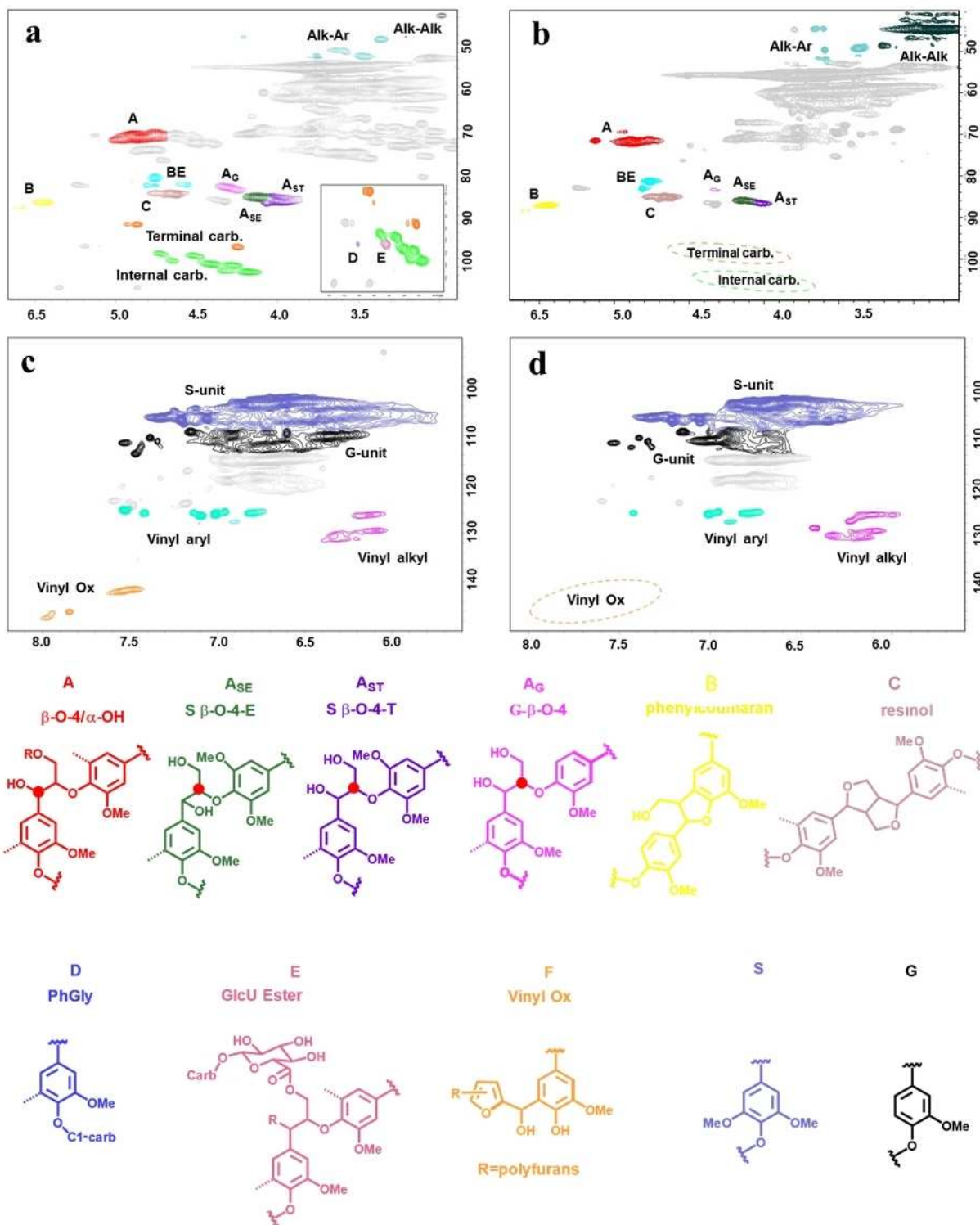


**Figure 3.** 2D HSQC NMR spectra of acetone extracted lignin at P-factor = 500 (a, c) and P-factor = 2500 (b, d). The liquid-to-solid ratio was set at 1 in both cases. The colored signals indicate the moieties of main interest quantified by the resonances of these signals.

main directions only. Based on Li et al. studies,<sup>[42]</sup> we assume that the cleavage of the main lignin moieties,  $\beta$ -O-4 structures, occurs via acid-catalyzed carbocation pathway leading to ether bond cleavage with the formation of Hibbert ketones and new

phenolic moieties or/and via radical cleavage (Scheme 1). The latter can result in the formation of cinnamyl alcohol structures, which undergo further transformations producing various olefinic moieties observed in much higher quantities than the

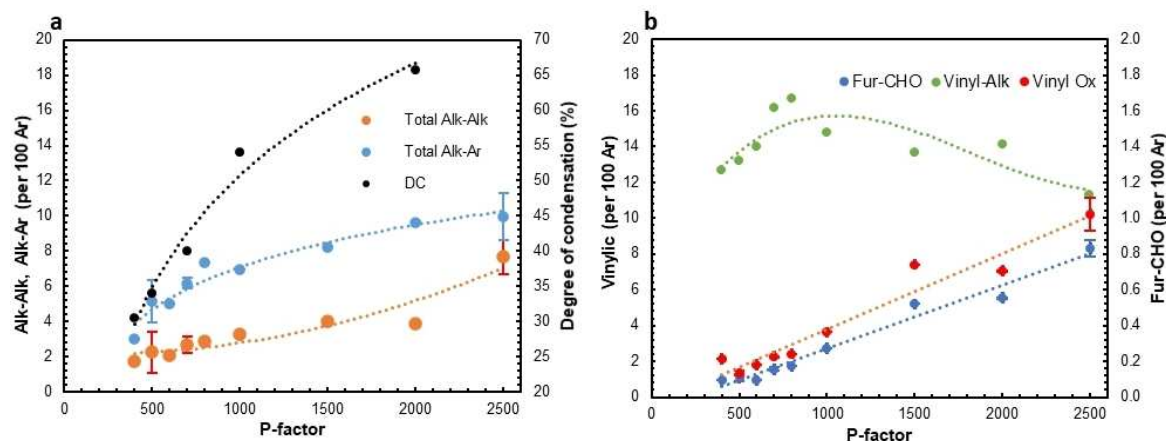


Figure 4. The effect of P-factor on the amount of different condensed moieties (a), vinylic and incorporated furan moieties (b) in AELs.

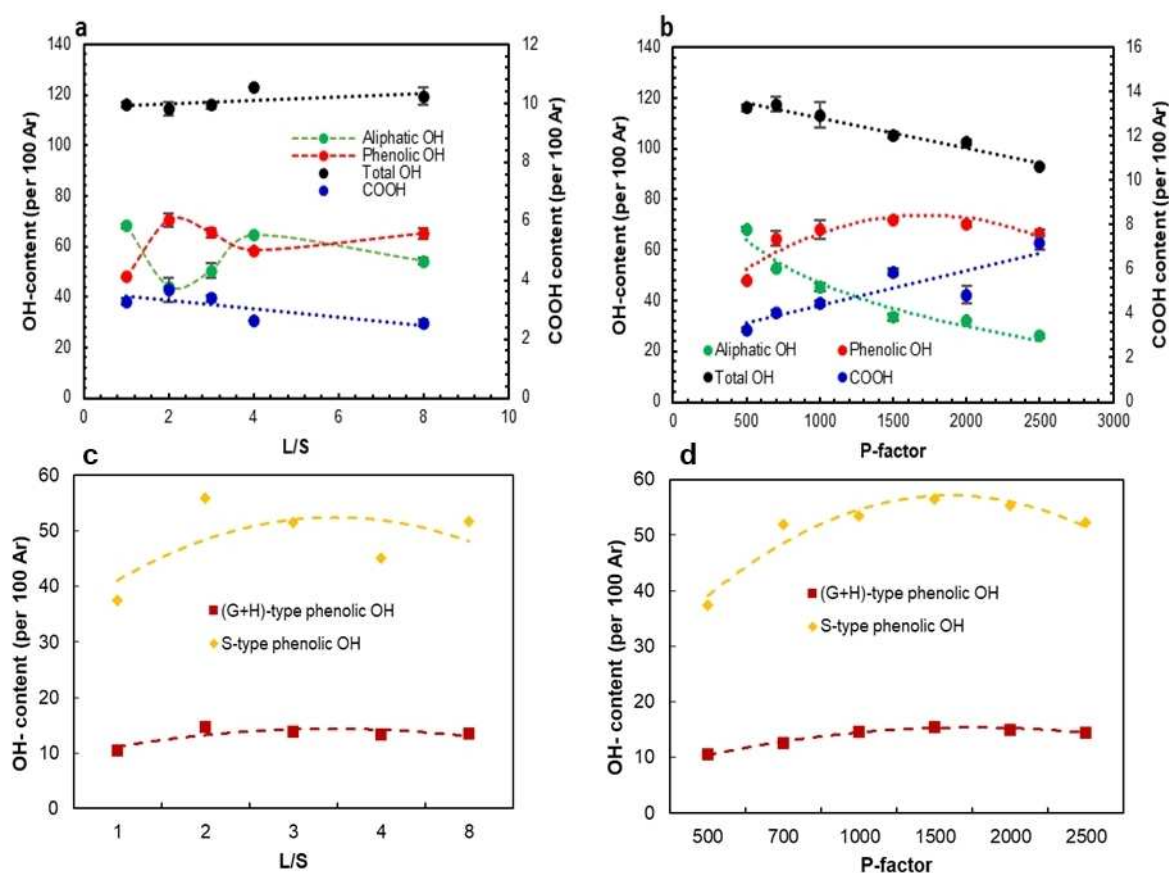
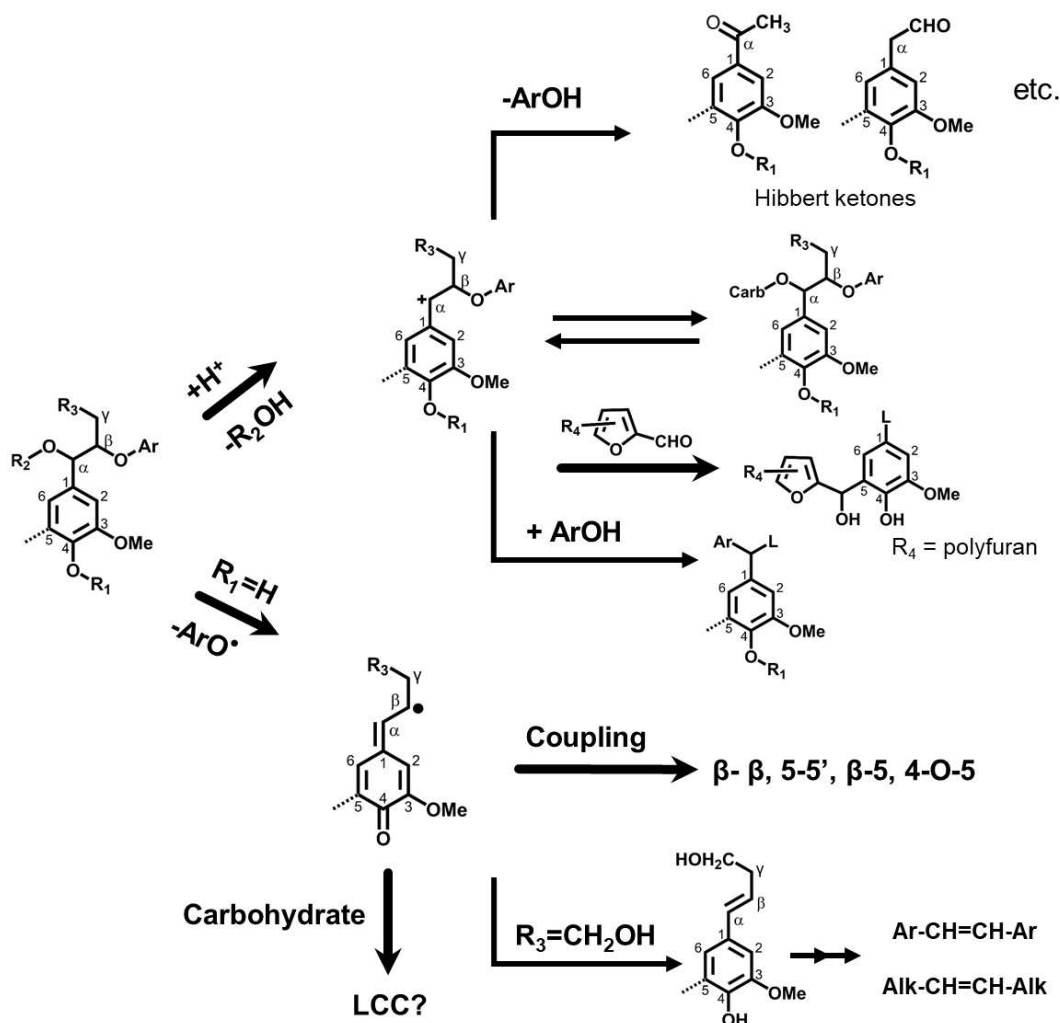


Figure 5. The effect of L/S ratio (a, c) and P-factor (b, d) on amount of different OH/COOH groups, determined by  $^{31}\text{P}$  NMR and corrected for carbohydrates contribution.

amount of cinnamyl alcohol structures. In addition, both carbocation and radical intermediates can undergo different condensation reactions forming new Alk-Ar (e.g.,  $\alpha$ -5,  $\alpha$ -6,  $\beta$ -5 types), Ar-Ar (e.g., 5-5' and 4-O-5' types) and Alk-Alk (e.g.,  $\beta$ - $\beta$  types) type of products. Noteworthy, the formed  $\beta$ -5 and  $\beta$ - $\beta$  structures were different from the original phenylcoumaran and resinol structures, as their abundance decreased during the

process. Furthermore, furan moieties of the furfural origin can be incorporated into the lignin structure predominantly via their carbonyl group.

As discussed above, reactions of LCC linkages play an important role in the process. The original LCC linkages can be cleaved under acidic conditions, for example, by hydrolysis of benzyl ether LCC forming the carbocation. However, this



**Scheme 1.** General direction of lignin and LCC transformations under AqSO process conditions.

reaction can be reversible when the carbocation reacts with available carbohydrates forming new LCC linkages (Scheme 1). Formation of new  $\gamma$ -ester linkages and especially PhGly moieties under the reaction conditions is very likely as evidenced by their very high abundance at low severity and L/S.<sup>[8]</sup> Apparently, mainly low molecular mass hemicelluloses (of high mobility) participate in the formation of the new LCC linkages thus making the newly formed LCCs soluble in water (hydrolysate) or aqueous acetone fractions. Further discussion on LCCs in different streams is present in our previous paper.<sup>[8]</sup>

It is of interest to discuss the propagation of these reactions, too. While the quantity of  $\beta$ -O-4 moieties exponentially decreased during the process, this did not correlate with the amounts of carbonyl and saturated aliphatic moieties, i.e., Hibbert ketones and other degradation products. Although significant quantity of these moieties was formed even in the earlier stages ( $P=400$ ), their amounts in AELs did not increase with increasing severity. It should be noted that AELs represent only 30–40% of the total lignin (about 60% of lignin remains in the solids) at low severity ( $P$ -factor < 600) while AELs in the

high severity range represent the majority of the total lignin. Therefore, the lack of changes in specific functionalities does not mean that the corresponding reactions do not occur in the whole lignin, but rather describes the structure of the acetone soluble fraction. As only minor amounts (1–2%) of cinnamyl alcohol moieties were detected in AELs they should be considered as reactive intermediates rather than the final reaction products. Apparently, further transformation of cinnamyl alcohol structures resulted in the formation of more complex olefinic moieties detected in much higher amounts. However, their amounts in AELs did not significantly change during the process either. The only types of new reaction moieties which gradually increased in the process were various condensed moieties (Alk-Alk, Alk-Ar, etc.) as well as furan-type products. However, lignin condensation did not prevent its extractability by aqueous acetone, likely due to concomitant cleavage of LCC linkages.

## 2D HSQC and <sup>13</sup>C NMR data correlation for LCCs

As described in our previous paper,<sup>[8]</sup> low HTT severities ( $P \approx 400$ – $600$ ) and low L/S resulted in AELs with the highest carbohydrate content, while an increase of P-factor and L/S resulted in the degradation of LCC linkages and higher degree of condensation (DC). Based on this observation, the discussion concerning LCC linkages will be focused on AELs obtained at low severity and L/S. As suggested by our group,<sup>[43]</sup> to have reliable quantitative data on the quantification of LCCs one should combine 2D HSQC and quantitative <sup>13</sup>C NMR techniques. At P-factor = 400 and L/S = 1, from HSQC and <sup>13</sup>C data, the total carbohydrate content in AELs was 27.6/100 Ar and 29/100 Ar, respectively, showing good correlation between the two techniques (Tables 1–3). Data correlated well between HSQC and <sup>13</sup>C also when P-factor was set in the range 500–700. A total carbohydrate amount of 17.3 vs. 15/100 Ar, and 15 vs. 15/100 Ar were determined at P-factors 500 and 700, by HSQC and <sup>13</sup>C, respectively (Tables 1 and 2).

## Outlook

To conclude, we present a short perspective on how such comprehensive structural information of AquaSolv Omni (AqSO) lignins can be beneficial for their engineering in specific applications. Our point of view about AqSO biorefinery has been thoroughly given in our previous paper.<sup>[8]</sup> In the present work we further discuss the issue based on the info herein reported.

AqSO process allows for selecting the most suitable processing parameters (P-factor and liquid-to-solid ratio) to achieve the desired lignin structure and properties. In other words, AqSO may be defined as a custom-designed, tunable type of biorefinery by which it is possible to produce different lignins (and products) through a simple variation of the reaction parameters. In AqSO process, a hydrothermal pretreatment has been upgraded into a novel biorefinery concept, of which the scope can be extended to other biomass feedstocks. The extraction of lignins after the (tunable) hydrothermal treatment using acetone as a green solvent with low boiling point (56 °C) is among the major strengths of the process. This makes the isolation of the extracted lignins viable by simple acetone evaporation, with no need for additional precipitation/filtration steps usually required in biorefinery.

The high variability in chemical structure, and hence physical properties reported earlier,<sup>[8]</sup> opens a plethora of opportunities to valorize AqSO lignins in a wide range of applications. To name few examples, lignins obtained at low severities with high  $\beta$ -O-4 content are suitable for their valorization through catalytic depolymerization, so called “lignin-first” approach, towards biofuels and chemicals.<sup>[44]</sup> On the other hand AELs produced at high severity, with high degree of condensation and molecular weight, and lower glass transition temperature ( $T_g$ ),<sup>[8]</sup> can find a better spot as wood adhesives, in various polymers blends for thermoplastics/thermosets, and as precursor for carbon fibers and activated carbons.<sup>[7]</sup>

In addition, the analytical methodology presented in this study can be used as basis for fast inline analytics in combination with AI-driven machine learning to ensure a reliable advanced biorefinery, as we have recently shown.<sup>[36]</sup> As structure-properties-performance correlation is a tough task to address considering the complex and irregular nature of lignin, AI-guidance would be a smart tool to be exploited in lignin engineering. In that regard, a novel fingerprint approach able to correlate AqSO lignins structure to their performance is currently under investigation in our group.

Furthermore, certain lignin moieties, such as different types of condensed structures, especially olefinic structures, and lignin-furan-moieties which have been tentatively assigned, are of high importance for wood/lignin biorefinery in general. Indeed, a holistic and comprehensive picture of the reactions involved in different pulping processes is still not available. For that reason, we are confident that our work enables new scenarios and pathways to be considered as key steps of well-established and high severity pulping methods, such as Kraft, and organosolv pulping, as well as during autohydrolysis and/or hydrothermal treatments (pre-)treatments of wood.

A structural comparison of AEL2000, Indulin, Alcell, and MWL lignins is given (Table 4). The label AEL2000 is referred to the AqSO acetone soluble lignin (AEL) obtained from a reaction in which P-factor and L/S are set at 2000 and 1, respectively. It is clear that certain structural features of AqSO AEL2000 are comparable to the ones of Indulin and Alcell. The  $\beta$ -O-4 content in AEL2000 is quite similar to the others, as well as resinol and phenylcoumaran structures, while total -OH groups are higher. Such higher number of active sites may be beneficial in certain applications, such as the production of Kraft lignin-based thermosets via poly-esterification or other methodologies.<sup>[2,49]</sup> Furthermore, AEL2000 has a higher phenolic OH groups content with respect to all the references of Table 4. Since it is well

**Table 4.** Comprehensive <sup>13</sup>C analysis (combination of acetylated and non-acetylated samples) of AEL2000 vs reference lignins (per 100 Ar).

Moieties	AEL 2000 <sup>[a]</sup>	Indulin <sup>[41]</sup>	Alcell <sup>[41]</sup>	Birch MWL <sup>[51]</sup>
C <sub>0</sub> nc	11	7	15	3
CO <sub>0</sub> ncj	15	8	14	9
Total CO	25	15	29	12
COOR <sub>0</sub> nc	11	15	17	3
COOR <sub>0</sub> ncj	2	2	4	1
Total COOR	13	17	21	4
OH primary	25	31	19	73
OH secondary	20	18	14	56
Total Aliphatic OH	45	49	33	121
Phenolic OH	76	66	70	20
Total OH	121	115	103	150
OMe	126	81	103	177
S/G ratio	1.70	0	1.18	3.02
ArH	185	234	202	209
DC. %	51	66	44	15
$\beta$ -O-4	6	7	7	66
resinol	4	4	3	9
phenylcoumaran	2	4	3	3
Oxygenated Aliphatic	130	93	82	260
Saturated Aliphatic	100	109	149	...
carbohydrates	3	1	<1	<1

[a] Acetone soluble lignin obtained at P-factor = 2000 and L/S = 1.

known that phenolic OHs play a key role in the antioxidant properties of lignins,<sup>[50]</sup> AEL2000 are expected to perform better (or at least comparably) with respect to Alcell and Indulin.

## Conclusions

We herein report a comprehensive (2D heteronuclear single-quantum coherence, <sup>13</sup>C and <sup>31</sup>P) NMR characterization of AquaSolv Omni (AqSO) acetone soluble lignins (AELs) with very detailed assignments and quantifications of almost all lignin signals, some of them for the first time. Novel structures, like alkyl-alkyl and alkyl-aryl lignin bonds, and condensed furan units, have been hypothesized and tentatively assigned based on reported data and chemical shifts molecular models. This allowed us to formulate some plausible insights into AqSO biorefinery reaction mechanism.

The value of AqSO biorefinery is found in its tunability, which allows for the isolation of different lignins with various structural features by simply varying the reaction parameters. For instance, at low severity and low liquid-to-solid ratio (L/S) less degraded lignins with high β-O-4 content (up to 34/100 Ar) were achieved and higher severities led to a more condensed lignin structure. Additionally, as thoroughly discussed in our previous paper,<sup>[8]</sup> AqSO gives the opportunity to achieve value from all major biomass components, through different streams bearing lignin, cellulose and hemicellulose valorization.

Overall, the comprehensive characterization of AqSO biorefinery lignins is a step forward towards lignin engineering for high value applications and can be useful for other biorefinery processes as well.

## Experimental Section

### Materials and chemicals

Acetone (C<sub>3</sub>H<sub>6</sub>O, 95 vol%), sulfuric acid (H<sub>2</sub>SO<sub>4</sub>, 98 wt. %), chromium (III) acetylacetonate, (Cr(acac)<sub>3</sub>), endo-n-hydroxy-5-norbornene-2,3-dicarboximide (e-HNDI), 2-chloro-4,4,5,5-tetramethyl-1,3,2-dioxaphospholane (TMDP), deuterated dimethyl sulfoxide (DMSO-d<sub>6</sub>), deuterated chloroform (CDCl<sub>3</sub>), and pyridine (all analytical grades) were purchased from Sigma-Aldrich.

### Sawdust preparation

Prior to hydrothermal treatment, Silver birch (*Betula pendula*) chips were finely ground (mean particle size 0.6 mm) with Wiley mill (Arthur H. Thomas Company). Then, the sawdust was screened (0.55–0.125 mm particle size) and air-dried. To eliminate the effect of lipophilic extractives, the sawdust underwent acetone Soxhlet extraction. In a typical procedure, the Soxhlet (containing a cellulose thimble) was filled with 50 g of screened and air-dried sawdust, and 200 mL of solvent (acetone). After refluxing for 24 h, the extracted sawdust was collected and air dried.

### AquaSolv Omni (AqSO) process

Hydrothermal treatment (HTT) of the extractive-free sawdust was carried out in a swing reactor, equipped with temperature control

in both heating block and inside the reactor, at 195 °C and at a liquid to solid ratio (L/S) in the range 1–8, following the procedure reported in our previous work.<sup>[8]</sup> As the heating period had significant effect on the course of the process, the severity of HTT was expressed as process severity (P-factor) as follows [Eq. (1)], assuming activation energy as 125.6 kJ/mol,<sup>[48]</sup> where *k* in the rate constant, *t* is the residence time (h) and *T* is the reaction temperature (K).

$$P\text{-factor} = \int_0^t \frac{k(T)}{k_{100\text{ }^\circ\text{C}}} dt = \int_0^t e^{40.48 - \frac{15106}{T}} dt \quad (1)$$

In a typical experiment, birch wood sawdust (4.21 g with 4.90% moisture content corresponding to 4.00 g o.d. wood) was placed inside the reactor together with the required amount of deionized water (3.8–32 g) to reach a liquid-to-solid ratio (L/S) in the range 1–8. The reactor was set to react until the required P-factor was reached (400–2500). Once the reaction was complete, the reactor was cooled down and the resulting hydrothermal treated biomass was separated by filtration and exhaustively washed with deionized water (200 mL) to achieve a hydrolysate liquor with pH ca. 4 and treated solids. The solids were then exhaustively extracted with non-toxic acetone (75% v/v, aq.), which maximized the yield of the extracted lignins when compared to another green solvent like ethanol (Table S1 and Ref. [8]). The low boiling point (56 °C) of acetone allowed for a facile isolation of the acetone soluble lignins (AELs) by rotary evaporation (*T* = 40 °C, *p* = 20 mbar), followed by high vacuum oven drying to constant mass at 40 °C over P<sub>2</sub>O<sub>5</sub> (*p* = 5 mbar). For a more detailed experimental procedure refer to our previously reported work.<sup>[8]</sup>

### Nuclear magnetic resonance (NMR) spectroscopy

**General.** The heteronuclear single-quantum coherence spectra were recorded with a Bruker AVANCE 600 NMR spectrometer equipped with a CryoProbe, while the <sup>31</sup>P and <sup>13</sup>C NMR spectra were recorded on a Bruker AV III 400 MHz.

### Heteronuclear single-quantum coherence (HSQC) NMR method

About 80 mg of sample was dissolved in 0.6 mL DMSO-d<sub>6</sub>. The acquisition time of 77.8 ms was set for <sup>1</sup>H-dimension and 36 scans per block were collected using the 1024 collected complex points. For <sup>13</sup>C-dimension, the acquisition time was 3.94 ms and 256-time increments were recorded. The 2D HSQC NMR data was manipulated with 1024 × 1024 data points applying the Qsine function for both <sup>1</sup>H and <sup>13</sup>C dimensions. The DMSO peak at δ<sub>C</sub>/δ<sub>H</sub> 39.5/2.49 ppm/ppm was used for calibration of the chemical shifts. The cross-peaks were assigned based on the previous reports.<sup>[43,49–52]</sup> The quantity of different lignin and LCC signals was normalized using the assumption [Eq. (2)]:

$$G + S = G_2 + S_{2,6}/2 = 100Ar \quad (2)$$

This assumption implies that the condensation (substitution) at the positions of G<sub>2</sub> and S<sub>2,6</sub> of lignin is insignificant, which will be verified in more comprehensive NMR studies. However, it is still valuable for relative comparison with the literature data as this normalization is used when only HSQC spectra of lignins are available.<sup>[43,50]</sup>

### <sup>31</sup>P NMR

The amounts of different hydroxyl groups were determined by <sup>31</sup>P NMR spectroscopy<sup>[53]</sup> in accordance with the optimized protocol.<sup>[54]</sup> The acquisition time and the relaxation delay were 1 s and 5 s, correspondingly; 128 scans were collected. Dry lignin samples (40.00 mg) were dissolved completely in a 1.6/1 (v/v) pyridine/CDCl<sub>3</sub> solution (0.4 mL) in a 5 mL vial. To this mixture, an internal standard (IS) solution (100 μL) of endo-N-hydroxyl-5-norbornene-2,3-dicarboximide (e-HNDI) in 1.6/1 (v/v) pyridine/CDCl<sub>3</sub> (C = 20 mg/mL) was added (IS:lignin = 0.3 μmol/mg) together with 50 μL of a relaxation agent Cr(acac)<sub>3</sub> solution in 1.6/1 (v/v) pyridine/CDCl<sub>3</sub> (C = 11.4 mg/mL). Then, 100 μL of phosphitylation reagent (2-chloro-4,4,5,5-tetramethyl-1,3,2-dioxaphospholane) were added to the mixture, which was stirred vigorously. The obtained solution was transferred into an NMR tube and <sup>31</sup>P NMR experiment was performed.

**Correction of <sup>31</sup>P NMR data for the presence of carbohydrates:** the calculation is based on an “average” molar mass for carbohydrates derived from composition (%) by methanolysis and by assuming 2 OH/mol (monomer unit) according to Equation (3).

$$X_{\text{corr}} = \frac{x - \text{carb} \cdot 10 \cdot \frac{2}{M_{\text{avcarb}}}}{100 - \text{carb}} \cdot 100 \quad (3)$$

Where:

$X_{\text{corr}}$  = the OH content corrected for the presence of carbohydrates.

$\text{carb}$  = carbohydrate content (%) determined by methanolysis

$M_{\text{avcarb}}$  = average molar mass of the carbohydrate fraction based on carbohydrate composition (%) from methanolysis analysis (approx. 163 g/mol).

### Quantitative <sup>13</sup>C NMR

The lignin samples (each about 200 mg) were dried in a vacuum-oven (temperature 40 °C) over P<sub>2</sub>O<sub>5</sub>. The dried lignins were dissolved in 0.55 mL of DMSO-*d*<sub>6</sub> containing a relaxation reagent, chromium(III) acetylacetonate (6 mg/mL). Once the sample was fully dissolved, the viscous solution was carefully transferred to an NMR tube with a glass Pasteur pipette. The spectra were collected with a Bruker 400 MHz and inverse gate detection and a 90-pulse width were used for the quantitative <sup>13</sup>C NMR acquisition. The acquisition time was set to 1.2 s, the relaxation delay to 2 s, and the number of scans to 20000. The spectra were processed as described earlier.<sup>[41]</sup>

### Acknowledgements

Academy of Finland (grant 341596) for funding support. D.T. and D.R. gratefully acknowledges support from the Academy of Finland through the FinnCERES BioEconomy flagship.

### Conflict of Interests

The authors declare no conflict of interest.

### Data Availability Statement

The data that support the findings of this study are available from the corresponding author upon reasonable request.

**Keywords:** reaction mechanisms · lignin · NMR spectroscopy, integrated biorefinery · lignin-carbohydrate complexes

- [1] C. Wang, S. S. Kelley, R. A. Venditti, *ChemSusChem* **2016**, *9*, 770–783.
- [2] D. Di Francesco, D. Rigo, R. Baddigam, A. P. Mathew, N. Hedin, M. Selva, J. S. M. Samec, *ChemSusChem* **2022**, *15*, e202200326.
- [3] J. T. Sutton, K. Rajan, D. P. Harper, S. C. Chmely, *ACS Appl. Mater. Interfaces* **2018**, *10*, 36456–36463.
- [4] J. F. Kadla, S. Kubo, R. A. Venditti, R. D. Gilbert, A. L. Compere, W. Griffith, *Carbon* **2002**, *40*, 2913–2920.
- [5] J. Seo, H. Park, K. Shin, S. Hyeon, *Carbon* **2014**, *76*, 357–367.
- [6] <http://www.storaenso.com/en/search?page=1&phrase=lignode>.
- [7] M. Y. Balakshin, E. A. Capanema, I. Sulaeva, P. Schlee, Z. Huang, M. Feng, M. Borghei, O. J. Rojas, A. Potthast, T. Rosenau, *ChemSusChem* **2021**, *14*, 1016–1036.
- [8] D. Tarasov, P. Schlee, A. Pranovich, A. Moreno, L. Wang, D. Rigo, M. H. Sipponen, C. Xu, M. Balakshin, *Green Chem.* **2022**, *24*, 6639–6656.
- [9] J. Li, G. Henriksson, G. Gellerstedt, *Bioresour. Technol.* **2007**, *98*, 3061–3068.
- [10] G. Wang, H. Chen, *Sep. Purif. Technol.* **2013**, *105*, 98–105.
- [11] S. Sun, X. Cao, S. Sun, F. Xu, X. Song, R. Sun, G. L. Jones, *Biotech. Biofuels* **2014**, *7*, 1–12.
- [12] T. V. Lourencon, L. G. Greca, D. Tarasov, M. Borrega, T. Tamminen, O. J. Rojas, M. Y. Balakshin, *ACS Sustainable Chem. Eng.* **2020**, *8*, 1230–1239.
- [13] D. Tarasov, M. Leitch, P. Fatehi, *Cellulose* **2018**, *25*, 1377–1393.
- [14] R. H. Narron, H. M. Chang, H. Jameel, S. Park, *ACS Sustainable Chem. Eng.* **2017**, *5*, 10763–10771.
- [15] L. Testova, K. Vilonen, H. Pynnönen, M. Tenkanen, H. Sixta, *Lenzinger Ber.* **2009**, *87*, 58–65.
- [16] J. S. Gütsch, T. Nousiainen, H. Sixta, *Bioresour. Technol.* **2012**, *109*, 77–85.
- [17] I. Sumerskiy, A. Pranovich, B. Holmbom, S. Willför, *J. Wood Chem. Technol.* **2015**, *35*, 387–397.
- [18] N. Feng, L. Ren, H. Wu, Q. Wu, Y. Xie, *Carbohydr. Polym.* **2019**, *224*, 115130.
- [19] K. Yao, Q. Wu, R. An, W. Meng, M. Ding, B. Li, Y. Yuan, *AIChE J.* **2018**, *64*, 1938–1953.
- [20] N. Giummarella, M. Lawoko, *ACS Sustainable Chem. Eng.* **2017**, *5*, 5156–5165.
- [21] E. A. Capanema, M. Y. Balakshin, C. L. Chen, J. S. Gratzl, H. Gracz, *Holzforchung* **2001**, *55*, 302–308.
- [22] E. A. Capanema, M. Y. Balakshin, J. F. Kadla, *J. Agric. Food Chem.* **2004**, *52*, 1850–1860.
- [23] M. Trogen, N. D. Le, D. Sawada, C. Guizani, T. V. Lourençon, L. Pitkänen, H. Sixta, R. Shah, H. O'Neill, M. Balakshin, N. Byrne, M. Hummel, *Carbohydr. Polym.* **2021**, *252*, 117133.
- [24] M. Leschinsky, G. Zuckerstätter, H. K. Weber, R. Patt, H. Sixta, *Holzforchung* **2008**, *62*, 653–658.
- [25] J. Li, G. Gellerstedt, *Ind. Crops Prod.* **2007**, *7*, 175–181.
- [26] N. Zhang, N. Sathitsuksanoh, B. A. Simmons, C. E. Frazier, J. R. Barone, S. Rennecker, *RSC Adv.* **2016**, *6*, 30234–30246.
- [27] J. Kaur, A. K. Sarma, M. K. Jha, P. Gera, *Biotechnol. Rep.* **2020**, *27*, e00487.
- [28] A. Kumar, B. Biswas, R. Kaur, B. B. Krishna, T. Bhaskar, *Bioresour. Technol.* **2021**, *342*, 126016.
- [29] S. Yu, M. Xie, Q. Li, Y. Zhang, H. Zhou, *J. Energy Inst.* **2022**, *103*, 147–153.
- [30] S. Kaur, G. Zhao, E. Busch, T. Wang, *Org. Biomol. Chem.* **2019**, *17*, 1955–1961.
- [31] H. Wang, B. Wang, D. Sun, Q. Shi, L. Zheng, S. Wang, *ChemSusChem* **2019**, *12*, 1059–1068.
- [32] T. Q. Yuan, S. N. Sun, F. Xu, R. C. Sun, *J. Agric. Food Chem.* **2011**, *59*, 10604–10614.
- [33] B. Bujanovic, R. S. Reiner, S. A. Ralph, R. H. Atalla, B. Bujanovic, R. S. Reiner, S. A. Ralph, R. H. Atalla, B. Bujanovic, R. S. Reiner, S. A. Ralph, R. H. Atalla, *J. Wood Chem. Technol.* **2011**, *31*, 121–141.
- [34] Z. Xia, L. G. Akim, D. S. Argyropoulos, *J. Agric. Food Chem.* **2001**, *49*, 3573–3578.

- [35] A. F. A. Wallis, in *Lignins Occur. Form. Struct. React.* (Eds.: K. V. Sarkanen, C. H. Ludwig), John Wiley & Sons, Inc, New York, **1971**, pp. 345–372.
- [36] J. Löfgren, D. Tarasov, T. Koitto, P. Rinke, M. Balakshin, M. Todorović, *ACS Sustainable Chem. Eng.* **2022**, *10*, 9469–9479.
- [37] M. Y. Balakshin, E. A. Capanema, 19 International Symposium On Wood, Fibre And Pulping Chemistry, Porto Seguro, **2017**, pp. 183–187.
- [38] N. Terashima, T. Akiyama, S. Ralph, D. Evtuguin, C. P. Neto, J. Parkäs, M. Paulsson, U. Westermark, J. Ralph, *Holzforschung* **2009**, *63*, 379–384.
- [39] E. A. Capanema, M. Y. Balakshin, J. F. Kadla, *J. Agric. Food Chem.* **2005**, *53*, 9639–9649.
- [40] T. M. Liitia, S. L. Maunu, B. Hortling, M. Toikka, I. Kilpeläinen, *J. Agric. Food Chem.* **2003**, *51*, 2136–2143.
- [41] M. Y. Balakshin, E. A. Capanema, *RSC Adv.* **2015**, *5*, 87187–87199.
- [42] S. Li, K. Lundquist, U. Westermark, *Nordic Pulp & Paper Research Journal* **2000**, *15*, 292–299.
- [43] M. Balakshin, E. Capanema, H. Gracz, H. min Chang, H. Jameel, *Planta* **2011**, *233*, 1097–1110.
- [44] M. M. Abu-Omar, K. Barta, G. T. Beckham, J. S. Luterbacher, J. Ralph, R. Rinaldi, Y. Román-Leshkov, J. S. M. Samec, B. F. Sels, F. Wang, *Energy Environ. Sci.* **2021**, *14*, 262–292.
- [45] X. Jiang, J. Liu, X. Du, Z. Hu, H. Chang, H. Jameel, *ACS Sustainable Chem. Eng.* **2018**, *6*, 5504–5512.
- [46] X. Lu, X. Gu, Y. Shi, *Int. J. Biol. Macromol.* **2022**, *210*, 716–741.
- [47] M. Y. Balakshin, E. A. Capanema, R. B. Santos, H. M. Chang, H. Jameel, *Holzforschung* **2016**, *70*, 95–108.
- [48] H. Sixta, *Pulp Properties and Applications* in Handbook of Pulp, Wiley, **2006**.
- [49] J. Ralph, L. L. Landucci, in *Lignin and Lignans* (Eds.: C. Heitner, D. Dimmel, J. Schmidt), CRC Press, Taylor & Francis, Boca Raton, **2010**, pp. 137–243.
- [50] M. Y. Balakshin, E. A. Capanema, C. L. Chen, H. S. Gracz, *J. Agric. Food Chem.* **2003**, *51*, 6116–6127.
- [51] C. S. Lancefield, H. J. Wienk, R. Boelens, B. M. Weckhuysen, P. C. A. Bruijninx, *Chem. Sci.* **2018**, *9*, 6348–6360.
- [52] M. Y. Balakshin, E. A. Capanema, H. M. Chang, *Holzforschung* **2007**, *61*, 1–7.
- [53] A. Granata, D. S. Argyropoulos, *J. Agric. Food Chem.* **1995**, *43*, 1538–1544.
- [54] M. Balakshin, E. Capanema, *J. Wood Chem. Technol.* **2015**, *35*, 220–237.

---

Manuscript received: April 18, 2023  
Revised manuscript received: May 22, 2023  
Accepted manuscript online: May 23, 2023  
Version of record online: July 17, 2023